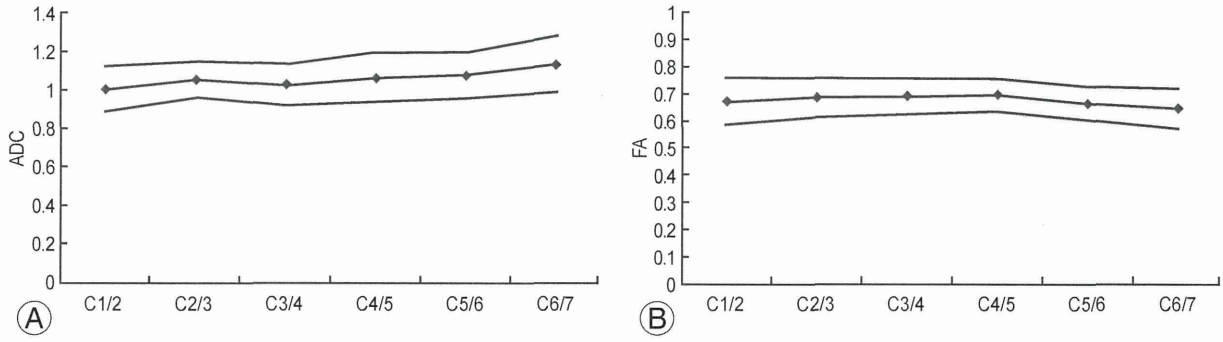

Fig. 3. **(A)** Apparent diffusion coefficient (ADC) (mean±standard deviation [SD]). **(B)** Fractional anisotropy (FA) (mean±SD).

There was no significant difference in FA values among the age groups (p=0.07) (Fig. 4C). Spearman rank correlation coefficient test showed that there was a weak negative correlation between FA and age, but it was not statistically significant (p=0.14) (Fig. 4D). Pearson correlation coefficient test showed that there was a weak negative correlation between ADC and FA values. However, the correlation was not statistically significant (p=0.07) (Fig. 4E). Moreover, although the ADC value tended to be higher in women, there was no significant difference in ADC values between men and women (p=0.24) (Fig. 4F). There was no significant difference in FA values between the two groups (p=0.051) (Fig. 4G); in addition, there was no significant difference in age between the 2 sexes (Fig. 5).

The mean percentage of ADC relative to the normal values at the C1/2 level was shown in Fig. 6A, and the mean percentage of FA relative to the normal ADC values at the C1/2 level was shown in Fig. 6B. Stable values were calculated for both parameters.

Discussion

Although some previous studies have compared parameters before and after surgery for compressive cervical disease using DTI [1,4,5], few have reported on normal values. Despite the influence of the imaging environment and individual differences on average ADC or FA values in healthy subjects [3,5], we obtained equivalent and stable normal values, as reported previously (Table 1) [3,6,7].

Mamata et al. [3] reported that in healthy subjects, ADC increased with age, whereas FA tended to decrease. In this study, as in previous reports, ADC was significantly higher in subjects >40 years of age; however, there was no significant difference in FA, and no difference between ADC and FA was found between men and women. It is expected that new trends will emerge as the number of cases increase.

Facon et al. [5] reported that a precise measurement is difficult to obtain because the value is affected by age, the measurement site, the imaging device, and the imaging method, even in a healthy spine. The relatively stable and reproducible values obtained in our study cases differed slightly from those previously reported, possibly due to the influence of these factors. To correct for individual differences, it is necessary to make comparisons with normal levels described in previous reports [8].

There are several reports on the usefulness of DTI. For example, Mamata et al. [3] reported that an increase in

Table 1. Comparison of the normal values of the ADC and FA with values in other reports

Study	No. of cases	ADC (μm^2/msec)	FA
Mamata et al. [3]	11	range, 0.75–0.81	0.66–0.75
Xiangshui et al. [6]	21	Mean±SD, 0.78±0.08	0.72±0.02
Takashima et al. [7]	10	1.03	0.64
Present study	31	1.06±0.09	0.68±0.05

ADC, apparent diffusion coefficient; FA, fractional anisotropy.

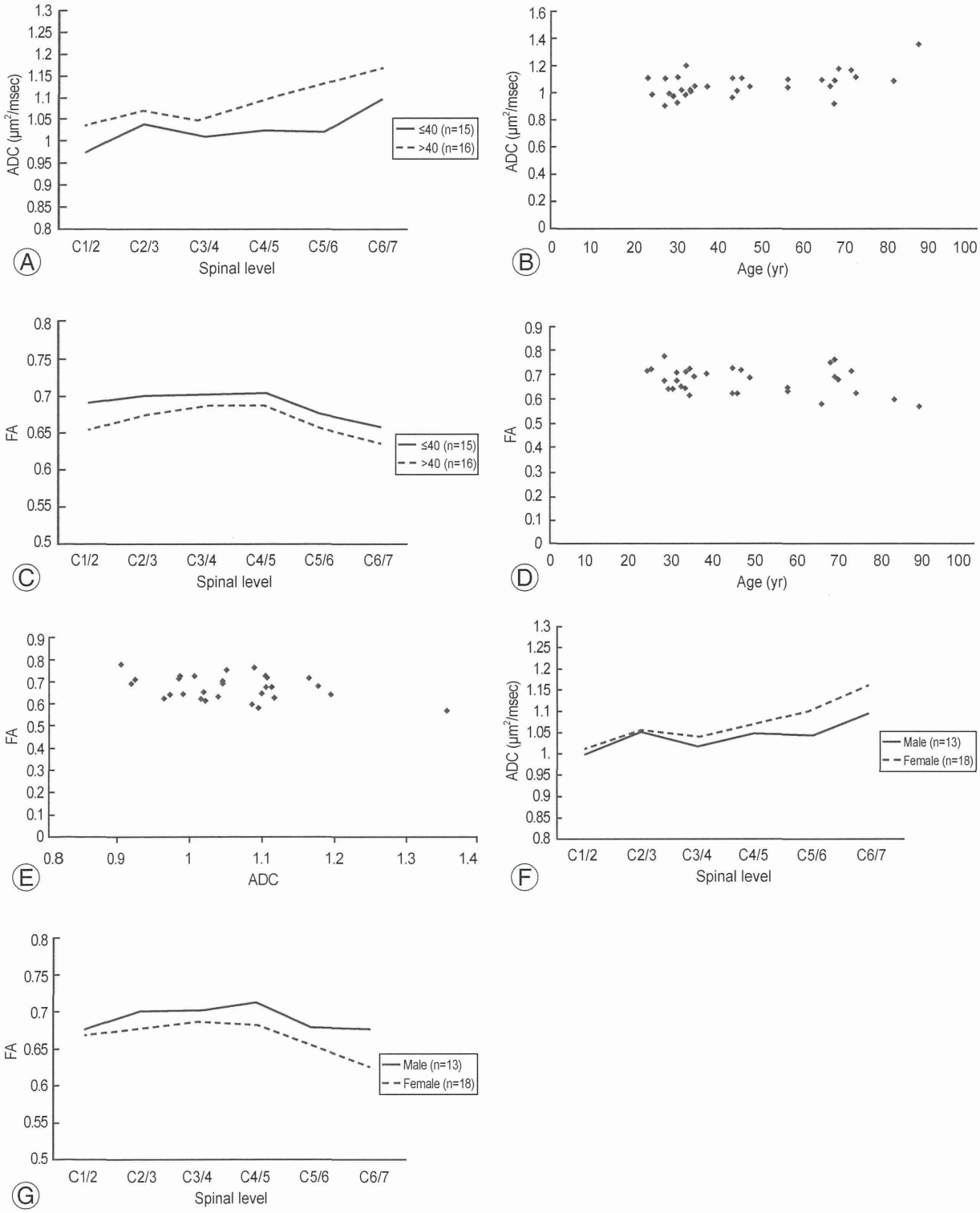

Fig. 4. **(A)** Apparent diffusion coefficient (ADC) was significantly higher in subjects >40 years of age than in those ≤40 years (p=0.04). **(B)** ADC was positively correlated with age by using Spearman rank correlation coefficient test (p=0.02). **(C)** Fractional anisotropy (FA) was not significantly influenced by age (p=0.07). **(D)** Spearman's rank correlation coefficient test showed that there was a weak negative correlation between the FA and age. However, the correlation was not statistically significant (p=0.14). **(E)** Pearson's correlation coefficient test showed that there was a weak negative correlation between the ADC and FA. However, the correlation was not statistically significant (p=0.07). **(F)** There was no significant difference in the ADC between males and females (p=0.24). **(G)** There was no significant difference in the FA between males and females (p=0.051).

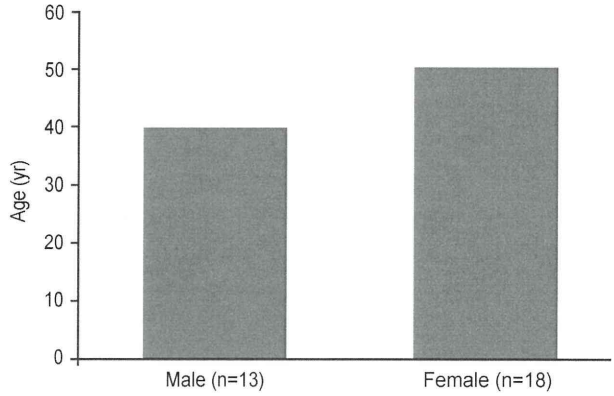

Fig. 5. There was no significant difference in the age between the two sexes.

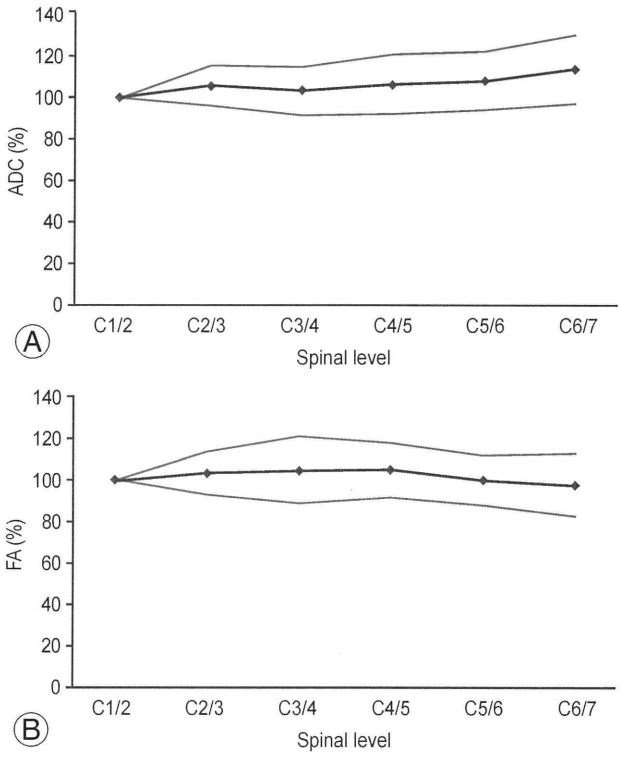

Fig. 6. **(A)** Percentage of apparent diffusion coefficient (ADC). **(B)** Percentage of fractional anisotropy (FA). Mean values indicate the percentage of the fractional anisotropy relative to the normal apparent diffusion coefficient values at the C1/2 level.

ADC and decrease in FA indicate the earliest stage of cervical spine disease; and Facon et al. [5] reported that a change in FA is extremely useful in detecting a spinal abnormality in the acute stage. Sei et al. [8] reported that FA and ADC correlated with several items included in the Japanese Orthopedic Association Cervical Myelopathy Evaluation Questionnaire, which suggested that these items can be used to quantify the severity of cervical spinal disease, whereas Wada et al. [1] reported that maintenance of the FA value before surgery may be an indicator of a good surgical outcome. Thus, DTI appears to be useful for the initial assessment of compressive cervical spinal disease or determining whether surgery is indicated. In addition, DTI can be used to quantify and evaluate the severity of cervical spondylotic myelopathy (CSM).

The normal ADC and FA values obtained in this study were stable and reproducible on axial views of several cervical levels and were easy to compare with abnormal values. Therefore, our findings should further contribute to the establishment of normal values. Further, the results of this study indicated that it is important to consider age and sex as DTI parameters and further suggested that measurements between each vertebral level are useful for diagnosis of impairment levels. We also found that comparing parameter values with normal levels contributed to a more accurate diagnosis of CSM. Future studies are required to confirm these results in larger numbers of healthy subjects and patients.

Conclusions

In this study, normal values of DTI parameters were identified in healthy subjects and were both reproducible and stable, which suggested that this method could be useful for patient assessment. Among the study participants, a significant difference was found only in the comparison of ADC by age; thus, it is important to consider age when evaluating cervical myelopathy. For diagnosis of impaired spinal levels, it is also important to consider the difference between the obtained and normal values at several levels.

Conflict of Interest

No potential conflict of interest relevant to this article was reported.

References

1. Wada A, Oda K, Kitagaki H, et al. Diffusion weighted and diffusion tensor imaging of the spinal cord. Sekitui Sekizui 2008;21:100-78.
2. Fujiyoshi K, Yamada M, Nakamura M, et al. In vivo tracing of neural tracts in the intact and injured spinal cord of marmosets by diffusion tensor tractogra-

phy. J Neurosci 2007;27:11991-8.
3. Mamata H, Jolesz FA, Maier SE. Apparent diffusion coefficient and fractional anisotropy in spinal cord: age and cervical spondylosis-related changes. J Magn Reson Imaging 2005;22:38-43.
4. Aota Y, Niwa T, Uesugi M, Yamashita T, Inoue T, Saito T. The correlation of diffusion-weighted magnetic resonance imaging in cervical compression myelopathy with neurologic and radiologic severity. Spine (Phila Pa 1976) 2008;33:814-20.
5. Facon D, Ozanne A, Fillard P, Lepeintre JF, Tournoux-Facon C, Ducreux D. MR diffusion tensor imaging and fiber tracking in spinal cord compression. AJNR Am J Neuroradiol 2005;26:1587-94.
6. Xiangshui M, Xiangjun C, Xiaoming Z, et al. 3 T magnetic resonance diffusion tensor imaging and fibre tracking in cervical myelopathy. Clin Radiol 2010;65:465-73.
7. Takashima H, Takebayashi Y, Yoshimoto S, Tuda H, Terashima Y, Yamashita T. Diffusion tensor imaging in cervical spinal cord by 3T MRI. J Spine Res 2011; 2;3:530.
8. Sei A, Kitajima M, Fujimoto T, et al. MR diffusion tensor imaging in cervical myelopathy. Sekizui Kinou Shindangaku 2009;31:65-9.

Kanchiku et al. BioMed Eng OnLine (2015) 14:98
DOI 10.1186/s12938-015-0094-5

BioMedical Engineering OnLine

RESEARCH Open Access

The efficacy of neuromuscular electrical stimulation with alternating currents in the kilohertz frequency to stimulate gait rhythm in rats following spinal cord injury

Tsukasa Kanchiku*, Hidenori Suzuki, Yasuaki Imajo, Yuichiro Yoshida, Atsushi Moriya, Yutaka Suetomi, Norihiro Nishida, Youhei Takahashi and Toshihiko Taguchi

*Correspondence:
tkanchik@yamaguchi-u.ac.jp
Department of Orthopedic Surgery, Yamaguchi University Graduate School of Medicine, Ube, Yamaguchi 755-8505, Japan

Abstract

Background: Rehabilitation facilitates the reorganization of residual/regenerated neural pathways and is key in improving motor function following spinal cord injury. Neuromuscular electrical stimulation (NMES) has been reported as being clinically effective. Although it can be used after the acute phase post-injury, the optimal stimulation conditions to improve motor function remain unclear. In this paper, we examined the effectiveness of NMES with alternating currents in the kilohertz (kHz) frequency in gait rhythm stimulation therapy.

Methods: Tests were performed using 20 mature female Fischer rats. Incomplete spinal cord injuries (T9 level) were made with an IH impactor using a force of 150 kdyn, and NMES was administered for 3 days from the 7th day post-injury. The needle electrodes were inserted percutaneously near the motor point of each muscle in conscious rats, and each muscle on the left and right leg was stimulated for 15 min at two frequencies, 75 Hz and 8 kHz, to induce a gait rhythm. Motor function was evaluated using Basso, Beattie, Bresnahan (BBB) scores and three-dimensional (3D) gait analysis. Rats were divided into four groups (5 rats/group), including the NMES treatment 75-Hz group (iSCI-NMES 75 Hz), 8-kHz group (iSCI-NMES 8 kHz), injury control group (iSCI-NT), and normal group (Normal-CT), and were compared.

Results: There was no significant difference in BBB scores among the three groups. In 3D gait analysis, compared with the injury control group, the 8-kHz group showed a significant improvement in synergistic movement of both hindlimbs.

Conclusion: We suggest that kHz stimulation is effective in gait rhythm stimulation using NMES.

Background

A moderate-to-high level of spinal cord injury generally presents with poor recovery of motor function. Improvement in function is limited when therapies are used alone, and a combination of several effective treatments may be required [1]. Rehabilitation promotes the intrinsic plasticity of the nervous system, which accelerates the recovery of motor function after incomplete spinal cord injury, and it is hoped that rehabilitation

will facilitate the reorganization of neural pathways after regenerative therapy [1]. Repetitive rhythmical movement of the legs facilitated by robot-assisted walking on a treadmill and combined with functional electrical stimulation therapy is clinically effective [2–4].

Neuromuscular electrical stimulation (NMES) has been used as a means of restoring limb motor function that has been lost primarily due to spinal cord injury and stroke. In experiments using monkeys, it has been found that, when part of the input/output pathway into the corticocerebral motor area is damaged, the functional map of the corticocerebral motor area undergoes plastic changes [5, 6]. In humans, studies using functional magnetic resonance imaging have shown that NMES-induced articular movement activates the brain area closer to automatic movement than that to hyperkinetic movement [7]; moreover, it has been reported that repetitive movement helps reorganize the functional map [8]. Thus, NMES is not simply a way to restore function but has also been used as a means of motor function training, the clinical effectiveness of which has been reported [3, 9–11]. However, the details of the mechanism that underlies the improvement in motor function remain unclear [12]. Basic research including animal experiments is needed to fully understand the mechanism of functional recovery and examine its effectiveness when combined with spinal cord regeneration therapies. However, there are relatively few reports on the effectiveness of rehabilitation combined with spinal cord regeneration therapies based on animal models. Therefore, this area needs to be explored further, including the development of suitable experimental animal models [1, 12].

Edgerton and Roy provided a detailed report of a treadmill gait-training animal model [13], whereas Courtine et al. reported that in a rat model of complete spinal cord injury, the combination of treadmill training, serotonergic agonists, and epidural electrical stimulation enabled weight-bearing treadmill locomotion [14]. However, treadmill-based gait training is performed during the chronic phase after spinal cord injury and is difficult to perform in the acute phase.

Jung et al. previously created electric stimulation models using rats as a model of functional NMES, in which they stimulated the motor points of the agonist muscles of the limbs using embedded electrodes. They also conducted a basic experiment to evaluate the stimulation conditions required to elicit synkinesia in each joint during gait [15–17]. As a result, they reported significant short-term improvements in the hindlimb synkinesia of rats with incomplete spinal cord injuries after NMES therapy [18]. NMES therapy can be used in the acute stage post-injury; however, in this model, electrodes are embedded, making it a highly invasive procedure. Therefore, a less invasive model is required to examine the effect of combined therapy in spinal regeneration.

Low-frequency pulsed currents (LPCs) and kilohertz-frequency alternating currents (KACs) are used to clinically augment muscle contractions. Treatment effectiveness may be enhanced by selecting stimulation parameters that evoke the strongest contractions with minimal discomfort and fatigue. Previous research findings regarding the muscle fatigue and degree of discomfort associated with KAC and LPC in patients with spinal cord injury are inconsistent [19, 20]. There is no report that investigates the effectiveness of NMES in stimulating gait rhythm using alternating currents in the kHz frequency for motor therapy.

We previously created a less invasive NMES therapy model using percutaneous needle electrodes and reported that kHz stimulation could be used for gait rhythm stimulation [21]. However, it is unclear whether NMES to stimulate gait rhythm using stimulation with alternating currents in the kHz frequency effectively improves motor function.

The purpose of the present study was to examine the effectiveness of using stimulation with alternating currents in the kHz frequency in improving motor function and to find the most effective NMES parameters available for gait rhythm stimulation after spinal cord injury.

Methods

Animals and study groups

This study was approved by the Committee for the Care and Use of Animals, Yamaguchi University (Yamaguchi, Japan). The protocols were designed and the study was conducted in accordance with the following regulations: Yamaguchi University Animal Regulations, laws on the care and maintenance of laboratory animals (Act no. 105); standards for the care and maintenance of experimental animals for the reduction of their suffering (Ministry of the Environment Public Notice no. 88); and basic policies on the use of animal experimentation at research institutions (Ministry of Education, Culture, Science, Sports and Technology Public Notice No. 7).

Twenty 12-week-old female rats (strain F334; Barcelona, Spain) weighing an average of 167 g (160–175 g) were used in this study. Thoracic spinal contusion injuries were induced in 15 rats, which were subsequently assigned to one of the following two groups: hindlimb movement therapy using NMES (iSCI-NMES, n = 10) or no treatment (iSCI-NT, n = 5). The NMES group was further divided into two groups on the basis of either a stimulation frequency of 75 Hz (iSCI-NMES 75 Hz, n = 5) or 8 kHz (iSCI-NMES 8 kHz, n = 5). Five rats that did not undergo training and in whom spinal cord injury was not induced were used as normal controls (Normal-CT, n = 5).

Creation of incomplete spinal cord injury

Rats were anesthetized with ketamine (25 mg) and xylazine (1 mg). A midline 2-cm incision was made to expose the spinal column at the 9th thoracic spine (T9) level, and the paravertebral muscles were bilaterally dissected to visualize the transverse apophysis. Laminectomy was carefully performed at the T9 vertebral arch without damaging the facets. A 150-kdyn contusion was induced in the rats using the Infinite Horizon spinal cord injury device (model IH-400®, Precision Systems and Instrumentation, LLC, Lexington, KY, USA). The surgical procedure was performed using a surgical microscope (Carl Zeiss AG, Jana, Germany). The wound was subsequently irrigated with saline solution, and the muscle, fascia, and skin were reapproximated. Post-surgery, 10 mL of 0.9 % sodium chloride and 10 mg of piperacillin sodium were subcutaneously injected. Access to food and water was facilitated in custom-built cages. Post-surgical care included manual bladder expression two times daily until bladder function resumed, as well as 10 mL injections of 0.9 % sodium chloride and 10 mg piperacillin sodium two times daily for 5 days.

NMES therapy

NMES was administered for 3 days from the 7th day post-injury (Fig. 1). Each rat was anesthetized and secured to a custom-made platform before stimulatory electrodes were percutaneously inserted into the tibialis anterior muscle and gastrocnemius muscle of both hindlimbs. To insert the electrodes near each motor point, anatomical motor point positions were referenced at the point of greatest contraction during post-percutaneous stimulation of the target muscle, using two different frequency currents (frequency, 75 Hz or 8 kHz; pulse width, 40 μs; amplitude, 1 mA; duration, 200 ms) [21].

Immediately after insertion of the stimulatory electrodes, strength–duration (SD) curves were generated for all muscles being studied [21] to assess whether the electrodes were positioned at appropriate target motor points. SD curves were constructed to show the relationship between the minimum current necessary to establish a stimulation threshold and pulse width. In this study, the minimum current necessary to cause visual muscle twitching was plotted by pulse widths of 20, 40, 60, 100, 200, and 500 μs per phase. The rheobase (the threshold twitch current over a prolonged pulse duration of 500 μs) and range of chronaxie (electrical current stimulus at the point where the threshold twitch current is twice the strength of the rheobase current and stimulates a muscle or neuron) were defined to assess the excitability of the muscle from the SD curves. Low rheobase and chronaxie values indicate that the electrode is positioned close to the motor point.

An isolated four-channel stimulator (STG2004®, Multi-Channel Systems, Cytocentrics, Reutlingen, Germany) was used in this study. The stimulation parameters were calibrated to those used in previous studies [15, 21]. The amplitude of the stimulation current was set at 1.5 times the threshold known to produce visually observable twitches. An automated four-channel patch clamp system, at a pulse width of 40 μs, was used. The timing of the muscle stimulations was matched to the walking rhythm of the right and left ankle agonists when a normal rat was walking on a treadmill [22]. Stimulations were performed for 15 min while the rats were conscious. To evaluate sequential changes in the articular range of motion (ROM) of the stimulated ankle joints, we performed three-dimensional (3D) kinematic analysis using the KinemaTracer® (Kissei Comtec Co., Ltd., Nagano, Japan). Color markers were attached to the joints of both hindlimbs (on the surface of the skin at the iliac region, hip, knee, ankle, and metacarpophalangeal joints). Four charge-coupled device video camera units were used to film these markers. Using

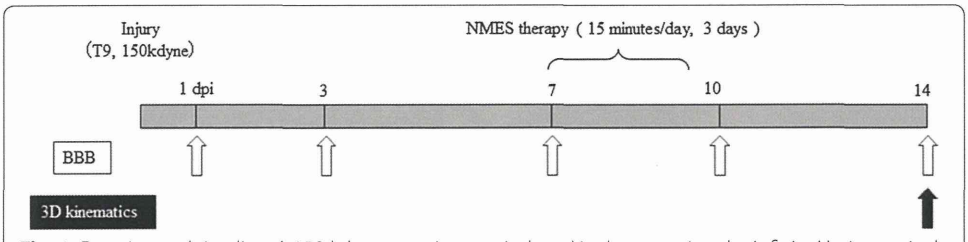

Fig. 1 Experimental timeline. A 150-kdyn contusion was induced in the rats using the Infinite Horizon spinal cord injury device at the 9th thoracic spine (T9) level. Neuromuscular electrical stimulation (NMES) therapy (15 min/day) was administered for 3 days from the 7th day post-injury. The Basso, Beattie, Bresnahan (BBB) locomotor rating scale was performed at 1, 3, 7, 10, and 14 days post-injury (dpi). A three-dimensional (3D) kinematic analysis was performed at day 14 dpi

kinematic analysis software, ROM was calculated and sequential changes were immediately evaluated at 5, 10, and 15 min post-stimulation (Fig. 2).

Assessment of locomotor coordination recovery

Overground walking locomotor score

Locomotion was assessed through open-field locomotor testing using the Basso, Beattie, Bresnahan (BBB) locomotor rating scale; this was performed at 1, 3, 7, 10, and 14 days post-injury (Fig. 1).

Hindlimb coordination during treadmill walking via kinematic analysis

Three-dimensional kinematic measurements, during treadmill walking 14 days post-injury (Fig. 1), were used to characterize intra- and interlimb coordination [18]. The analysis provided joint angle trajectories during the stance and swing phases as well as the touchdown (TD) and lift-off (LO) events during multiple gait cycles.

Rats were anesthetized with 2 % sevofrane. Hair was clipped around both the upper and lower limbs, and skin glue markers were placed over 16 anatomic landmarks on the bilateral side of the shoulder, elbow, wrist, iliac crest, greater trochanter, knee joint, lateral malleolus, and fifth metatarsal head. Hemispherical markers were prepared using 6-mm doll eyes that were air painted in blue, orange, red, green, and yellow, and then coated with bitter spices to keep the test rats from biting them. One operator performed all marker placements to avoid inter-tester variability. All rats were made to walk on a treadmill (MELQUEST Co.: TMC-100) at 13.7 cm/s, and results were recorded and analyzed using the Kinema Tracer® (Kissei Comtec Co., Ltd., Nagano, Japan), which was equipped with four high-speed digital cameras at 120 fps and controlled using IEEE1394 cables (Fig. 3). Kinematic data were collected at a sampling rate of 1000 Hz. This system can analyze stick pictures, time–distance factors, joint angles, joint acceleration, and Lissajous figures. The four cameras were positioned right and left anteriorly and right and left posteriorly. We used an original clear box (56 × 106 × 206 mm) for camera calibration that contained 18 calibration points with controls (corners and middles). As previously noted, rats were made to walk at treadmill speeds of 13.7 cm/s. Rotations per

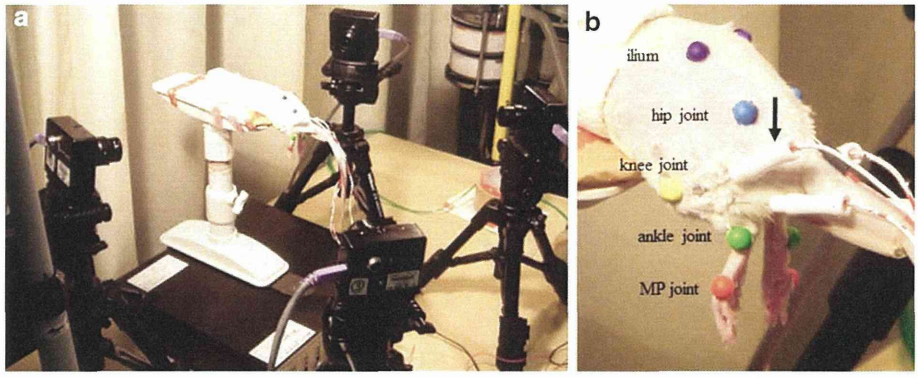

Fig. 2 Insertion of electrodes and setting of gait rhythm stimulation. Each rat was anesthetized and secured to a platform (**a**). Needle electrodes (*down arrow*) were percutaneously inserted into the tibialis anterior (TA) muscle and gastrocnemius (Gc) of both limbs (**b**). With the rat awake and the trunk secured, gait rhythm was stimulated using stimulation electrodes and filmed using four charge-coupled device cameras (**a**)

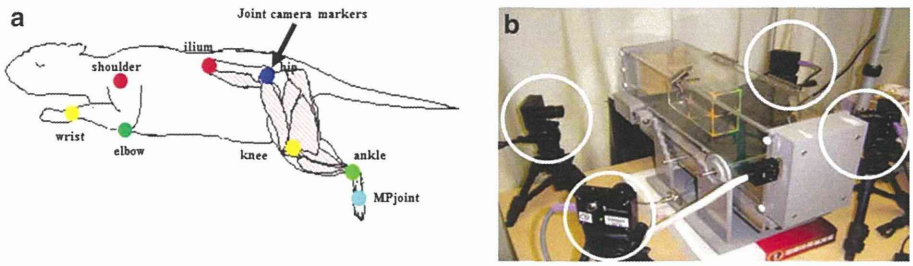

Fig. 3 Three-dimensional gait analysis. Camera markers were attached to each joint of the four limbs, and the rat was made to walk at a set speed on the treadmill. The camera markers (*down arrow*) (**b**), which were attached to the lower limbs, were filmed using four charge-coupled device cameras (*unfilled circle*) (**a**), and the digital data obtained was analyzed and evaluated

minute on the treadmill were calculated at 0.273 cm/s; thus, 50 rpm equaled 13.7 cm/s. The images were recorded for 11 s, which is the maximum time allowed by the system.

The video frame, in which the hindlimb toes of a rat touched the treadmill belt, was recorded as a touchdown (TD) event. Similarly, a liftoff (LO) event was marked when a rat's hindlimb toes lifted off the treadmill belt. This approach for marking the TD and LO events has been used to describe gait kinematics in a previous report [22]. A step cycle was considered to be the duration from right TD to right TD. Each cycle was normalized to 100 % and calculated on a cycle-by-cycle basis.

Normalized joint angle trajectories and joint angle–angle plots for right and left ankle movements were used to assess intra- and interlimb coordination. Right–left symmetry during movement was quantitatively analyzed using the interlimb angle–angle plots [22]. Each normalized cycle is represented by 201 data points. A right ankle joint angle at any given point within a cycle, i (θRAi), can be used to predict the left ankle joint angle at i + 101 (θLAi + 101) for all points in the data set (the first 100 points from the first cycle of the right joint and the last 100 points from the last cycle of the left joint were discarded). The difference between the points and the line was then calculated to determine the symmetry error. The root mean square (RMS) error was calculated to characterize the entire normalized dataset with a symmetry index as follows:

$$SYM\_E = \sqrt{\frac{\sum_n \left(\frac{\theta RH_i - \theta LH_{i+101}}{\sqrt{2}}\right)^2}{n}}$$

Quantitative assessment of interlimb gait coordination was conducted to determine consistency of 1:1 correspondence between the right and left hindlimbs and to establish the relative phase of each limb TD with respect to another within a gait cycle. In this study, mean Φ and R values were calculated in a circular phase to assess the consistency of 1:1 hindlimb right–left interlimb coordination (Fig. 4). The mean Φ values were normalized to 0.5. Some dispersion was shown by the R values, with dispersion decreasing as the R value approached 1 and increasing as the R value approached 0. The mean Φ and R values were compared among the iSCI-NMES 75 Hz, iSCI-NMES 8 kHz, iSCI-NT, and Normal-CT groups.